Figure 2.4 (a) Energy levels of an electron spin as a function of a magnetic field. The resonance by microwave absorption occurs at $H_o = h\nu/g\beta$. (b) Electronic ground and excited levels and a transition induced by an optical absorption: E [eV] $= 1239/\lambda$ (λ is a wavelength in [nm]).
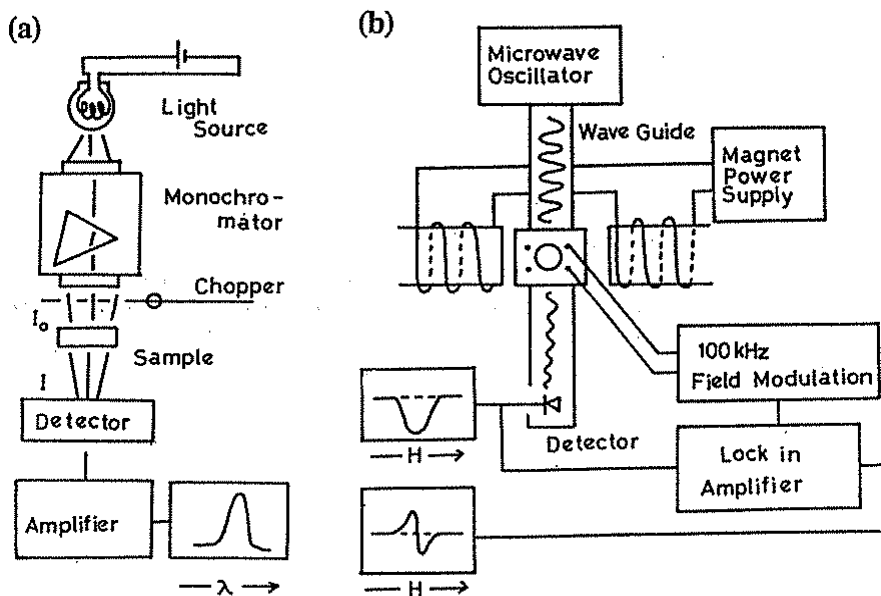

Figure 2.5 Analogical illustration of spectrometers for (a) optical absorption and (b) ESR measurement.
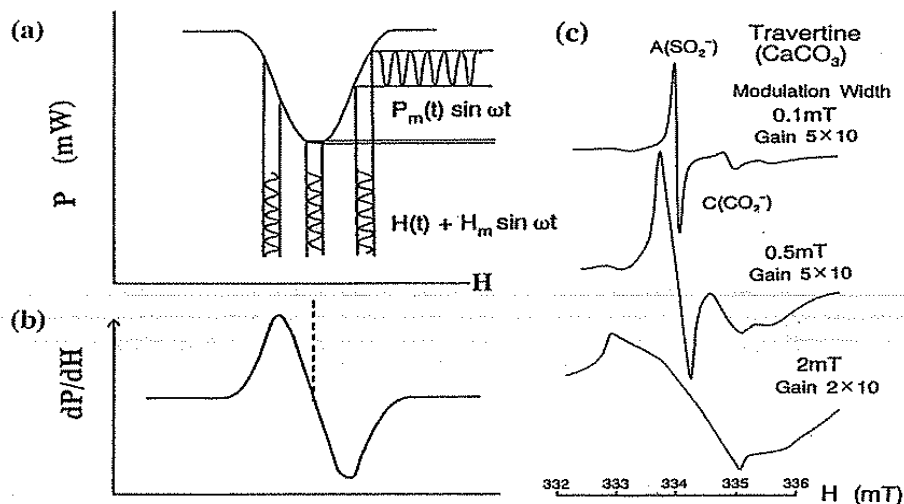
Figure 2.6 (a) The absorption curve and the magnetic field modulation method. (b) The ESR spectrum recorded in a form of the first derivative line as a function of the magnetic field, H. (c) ESR spectra of spring travertine (natural $CaCO_3$) with different modulation widths. Overmodulation larger than the linewidth of signals broadens the signals and distorts the line shape.

If the width of the ESR signal is 0.1 mT, one can detect a minimum number of $10^9 \sim 10^{10}$ spins in the sample with an ordinary spectrometer.

Table 2.2 Absorption and the first derivatives of Gaussian and Lorentzian lineshapes and the half–width ($\Delta H_{1/2}$), maximum slope width (ΔH_{msl}) and the average second moment as indicated ($<\Delta H^2>^{1/2}$) with theoretical spin–spin relaxation time (T_2).
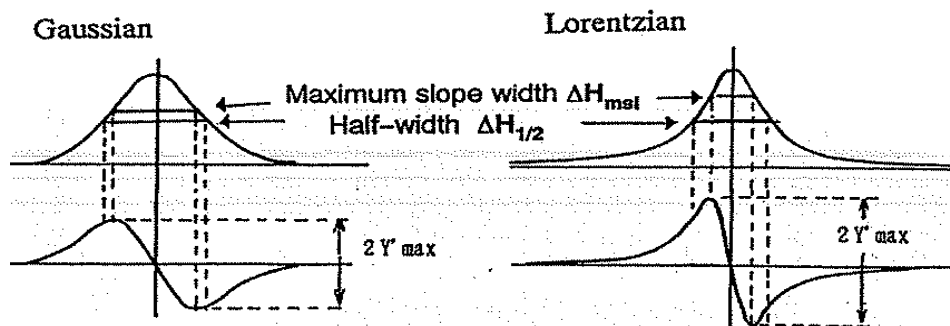
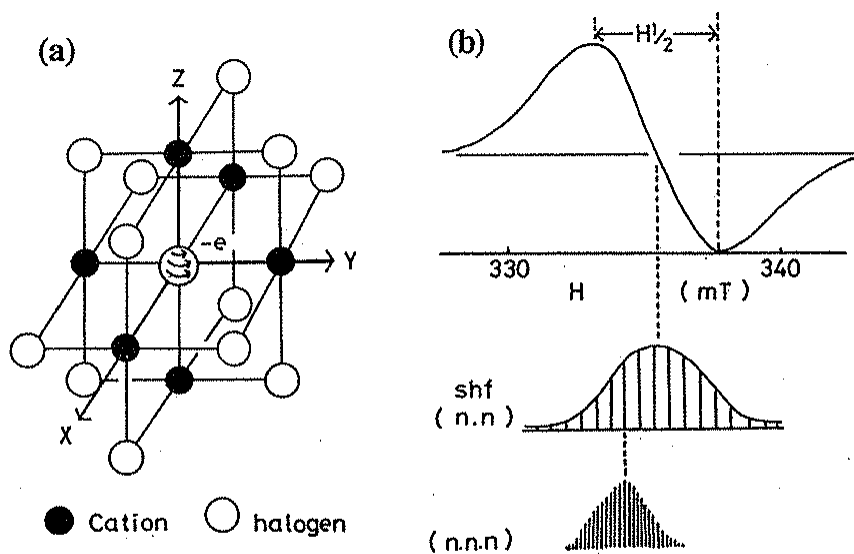| Lineshape	$\Delta H_{1/2}$	ΔH_{msl}	$<\Delta H^2>^{1/2}_{av}$	$\frac{\Delta H_{1/2}}{\Delta H_{msl}}$	$\frac{\Delta H_{1/2}}{<\Delta H^2>^{1/2}_{Ave}}$
Gaussian	$\left(\frac{\ln 2}{\pi}\right)^{1/2}\frac{1}{T_2}$	$\frac{1}{\sqrt{2\pi}\,T_2}$	$\frac{1}{\sqrt{8\pi}\,T_2}$	1.177	2.355
Lorentzian	$\frac{1}{\pi T_2}$	$\frac{1}{\sqrt{3}\,\pi T_2}$	∞	1.732	0

2

(a)

(b)

Figure 2.16 (a) A model of the F center in alkali halides and (b) ESR spectrum of the F center with the width due to shf by the nearest neighbor (n.n) alkali and next nearest neighbor (n.n.n) halogen ions (Seidel 1961).
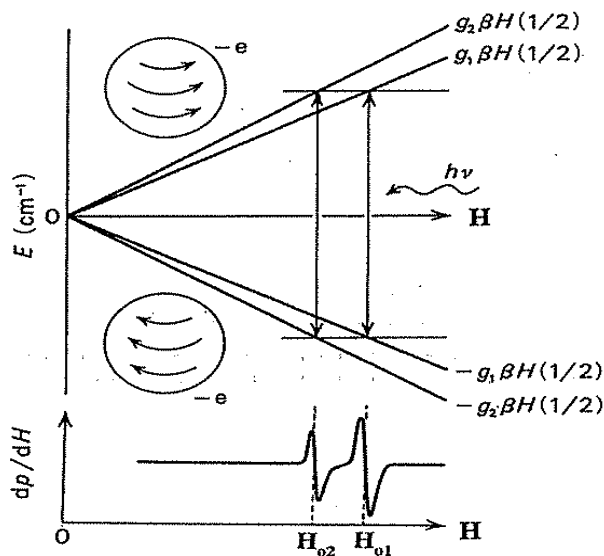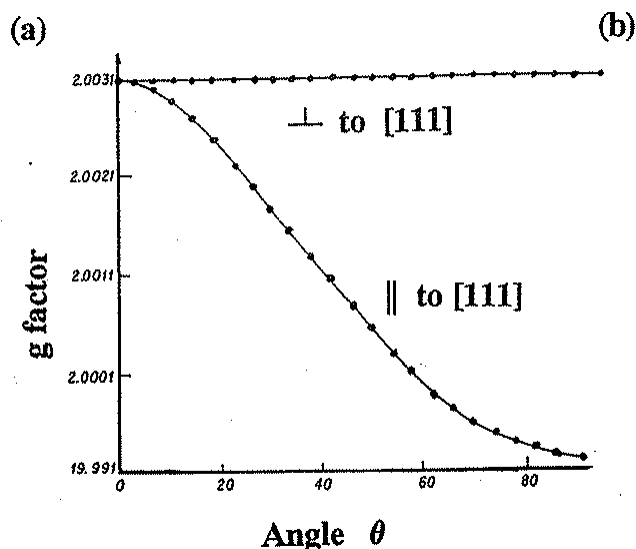
Figure 2.8 Energy levels of spins with two different g factors of g_1 and g_2. The magnitude of the magnetic moment or the interaction of the electrons with orbital magnetic moment through the spin–orbit interaction results in different g factors, i.e., different slopes in the energy level diagram. The absorption positions in the derivative form are shown below.

The g factors are generally around 2.0 and are usually determined to the fourth decimal place with a probable error of $0.0002 \sim 0.0005$. Free electrons have $g_e = 2.0023$ (rather than the classical value of 2.0000) due to relativistic correction. A radical with electron excess shows a g factor smaller than g_e. An electron–deficient radical (hole center) shows a g factor slightly larger than g_e i.e., the signal of a hole center appears at a lower magnetic field than that of a free electron. There is a proposal to use the third and fourth decimal figures by subtracting 2.0 from the g factor to identify a signal. The g factor would therefore be 23 for $g_e = 2.0023$. However, signals of $g = 1.9975$ or $g = 2.43$ are difficult to call in this notation. Hence, we describe the g factor using up to the fourth decimal place. It is possible to obtain g factors of high resolution at high microwave frequencies of Q– and K–bands ($\nu = 35$ and 25 GHz, respectively).

An ESR signal is identified by the g factor. The shift of the g factor from the free electron value ($g_e = 2.0023$) is caused by the spin–orbit interaction, λLS, of the electron in the atomic orbital, where λ is the *spin–orbit interaction parameter* and L is the *orbital magnetic moment* of the relevant

(a)　　　　　　　　　　　　　　(b)

Angle θ

(a) $(Mg,Fe)SiO_3$

Mn^{2+}

$M=+1/2 \leftrightarrow -1/2$

(b) $CaSiO_3$

$M=+5/2 \leftrightarrow +3/2$ $M=+3/2 \leftrightarrow +1/2$ $M=+1/2 \leftrightarrow -1/2$ $M=-1/2 \leftrightarrow -3/2$ $M=-3/2 \leftrightarrow -5/2$
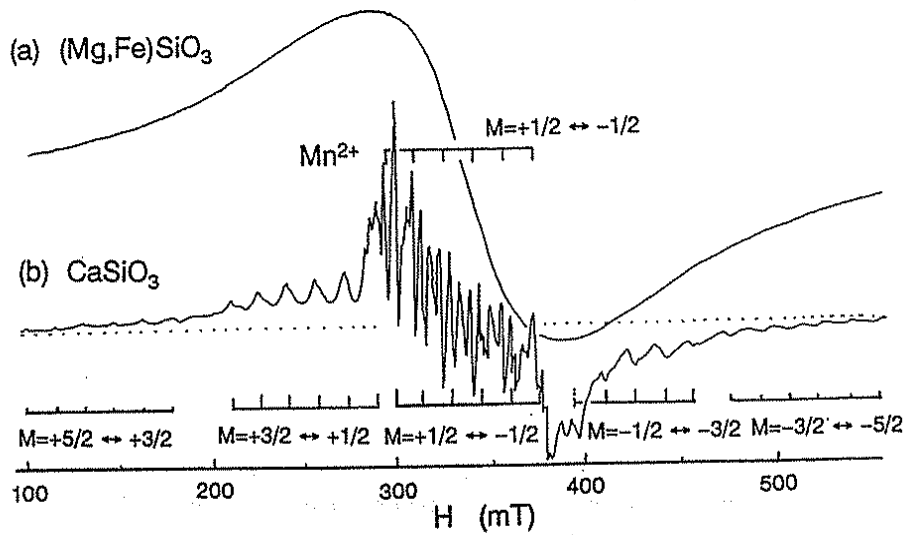
100   200   300   400   500

H (mT)

Figure 2.24 (a) One broad line is observed for $(Mg, Fe)SiO_3$ due to dipolar and exchange interactions of Mn^{2+} and Fe^{3+}. (b) ESR spectrum of Mn^{2+} in pyroxene $(CaSiO_3)$. The allowed and forbidden lines of hf splittings are associated with $\Delta M = \pm 1$, $\Delta m = 0$ and $\Delta M = \pm 1$, $\Delta m = \pm 1$, respectively.

Techniques and Materials

amino acid racemization
(bone collagen)

uranium series
(speleothems, shells, corals, bones)

obsidian hydration
(obsidian, volcanic glasses

archaeomagnetism   palaeomagnetism
(ceramic, brutned clay, kilns)

electron spin resonnance
(fossilisied bones, calcite formations)

thermoluminescence   optical luminescence
(pottery, sediments, mortars, slags)

dendrochronology
(trees)

radiocarbon
(wood, bones, sheeds, bones, paper)

10   100   1000

Age Range (in thousand years)